A Modified Artificial Potential Field using Perpendicular Force for Leader-Follower System

Gilang N. P. Pratama
Universitas Negeri Yogyakarta
Yogyakarta, Indonesia
gilang.n.p.pratama@uny.ac.id

Mentari P. Jati
National Taipei University of Technology
t111999402@ntut.edu.tw

Ardy S. Priambodo
Universitas Negeri Yogyakarta
Yogyakarta, Indonesia
ardyseto@uny.ac.id

Oktaf A. Dhewa
Universitas Negeri Yogyakarta
Yogyakarta, Indonesia
oktafagnidhewa@uny.ac.id

Arya Sony
Universitas Negeri Yogyakarta
Yogyakarta, Indonesia
arya.sony@uny.ac.id

***Abstract*—Artificial potential field (APF) is a path planning strategy that is widely used in robotics. Unfortunately, it is susceptible to local minima problems, especially on Symmetrically Aligned Robot-Obstacle-Goal (SAROG) configurations. In this paper, we propose a modified APF by introducing the perpendicular force for escaping the local minima. Furthermore, it is also being implemented for the leader-follower system. Here, the leader is assigned to reach the goal while avoiding obstacles. Simultaneously, the follower needs to track the leader while maintaining a safe distance. The effectiveness of our proposed method is verified by numerical simulations. The results show that the modified APF using perpendicular prevails in guiding the leader to reach the goal. At the same time, the follower can maintain a tolerated distance from the leader.**

***Keywords*—Modified Artificial Potential Field, Path Planning, Leader-Follower System, Perpendicular Force, SAROG.**

I. Introduction

Currently, autonomous robots are prevalent in various fields, including military applications, industries, and our daily life [1]. Researchers have shown increasing interest in this field over the years. One significant area of research in robotics is path planning, which involves determining the optimal route for a robot to navigate from its starting point to its destination [2]. Numerous path planning strategies exist for mobile robots, such as Dijkstra [3], artificial potential field (APF) [4], rapidly exploring random tree (RRT) [5], A-star [6], [7], and many more. Among these, APF stands out for its relatively low computational complexity, enabling real-time implementation. It is introduced by Khatib in 1985 [8], APF utilizes attractive and repulsive forces to guide the robot towards the goal while avoiding obstacles [9]. Despite its simplicity, traditional APF suffers from certain drawbacks. One of them is the fact that APF is susceptibility to local minima, where the total force becomes zero, potentially resulting in the robot getting trapped and unable to move [10]. Previous studies have been conducted for tackling those problems, including the research by Rizqi *et al*. [11] and Triharminto *et al*. [12]. They have attempted to modify the repulsive field to escape local minima. However, such modifications require extensive analysis and redefine the repulsive force [13].

In contrast to previous approaches [12]–[14], this research puts forth a proposition that modifies the path planning process by introducing an additional virtual force. This new force operates in conjunction with the established repulsive field but serves a distinct purpose by generating paths that diverge perpendicularly from obstacles. Furthermore, we also present a dynamic path planning for leader-follower scenario by using the modified APF. In this context, the primary objective is for the leader to reach its designated goal while avoiding the obstacles. Simultaneously, a path is generated for the follower to chase the leader while also ensuring obstacle avoidance. An important consideration is maintaining an adequate distance between the leader and follower.

The rests of this paper are as follows. A brief explanation of APF is presented in Section II. It covers the attractive, repulsive, and total force for leader and follower-robot. Later, in Section III, the local minima problem and the solution using perpendicular force are presented. After the necessaries, the results and analysis of this research can be found in Section IV. Last but not the least, the conclusion of our proposed mothod for leader-follower system using modified APF is presented in Section V.

II. Artificial Potential Field

As previously stated, the two main forces involved here are the attractive and the repulsive force. Our focus here is on designing potential fields within the two-dimensional space denoted as $\mathbf{C} \in \mathbb{R}^2$, which enables us to guide the robot reaches the goal while avoiding the obstacles. These obstacles, represented by $\mathbf{C}_{\mathbf{o}_i} \in \mathbb{R}^2$, occupy specific regions within the space.

A. Attractive Force

The attractive force attracts the leader-robot from the starting position to the designated goal. It is also used for the follower to chase the leader. Before proceeding any further,

979-8-3503-1563-9/23/$31.00 ©2023 IEEE

we need to establish some prerequisites. Firstly, we need to define the position of the leader-robot as $\mathbf{q}_l = \begin{bmatrix} x_l & y_l \end{bmatrix}^{\mathrm{T}}$, the position of follower-robot as $\mathbf{q}_f = \begin{bmatrix} x_f & y_f \end{bmatrix}^{\mathrm{T}}$, and the goal as $\mathbf{q}_g = \begin{bmatrix} x_g & y_g \end{bmatrix}^{\mathrm{T}}$. Now, we can define the vector direction towards the goal, $\mathbf{d}_g$, that can be denoted as

$$\mathbf{d}_g = \frac{\mathbf{q}_g - \mathbf{q}_l}{\|\mathbf{q}_g - \mathbf{q}_l\|}. \tag{1}$$

In equation (1), $\|\mathbf{q}_g - \mathbf{q}_l\|$ represents the magnitude of a vector difference between the position of the leader and the goal.

Simultaneously, there are two things that need to be determined for the follower. First, we need to calculate the distance between the leader and follower, which can be defined as

$$l = \sqrt{(x_l - x_r)^2 + (y_l - y_r)^2}. \tag{2}$$

The second thing that need to be determined is the direction of follower towards the leader, which can be denoted as

$$\mathbf{d}_l = \frac{\mathbf{q}_l - \mathbf{q}_f}{\|\mathbf{q}_l - \mathbf{q}_f\|}, \tag{3}$$

In equation (3), $\|\mathbf{q}_l - \mathbf{q}_f\|$ represents the magnitude of a vector difference between the position of the follower and the leader.

After obtaining the vector directions, we can determine the attractive force for leader-robot $\mathbf{F_{a1}}$ and the attractive force for follower-robot $\mathbf{F_{a2}}$. The attractive force for the leader-robot can be denoted as

$$\mathbf{F_{a1}} = k_{a1}\mathbf{d}_g, \tag{4}$$

where k_{a1} is the attractive gain for the leader-robot. Meanwhile the attractive force for follower-robot can be expressed as

$$\mathbf{F_{a2}} = \begin{cases} k_{a2}\mathbf{d}_l & \text{, if } l \geq l_s, \\ 0 & \text{, otherwise,} \end{cases} \tag{5}$$

where k_{a2} is the constant attractive gain for the follower-robot. Meanwhile, l_s is the allowed minimum distance between the leader and follower.

B. Repulsive Force

The repulsive force plays an important role in avoiding obstacles encountered during path generation. It has to repel the leader-robot from the obstacles and the follower-robot. Simultaneously, the repulsive force also needs to repel the follower-robot from the obstacles. In order to achieve those feats, we need to define the vactor position of the obstacle as $\mathbf{q}_o = \begin{bmatrix} x_o & y_o \end{bmatrix}^{\mathrm{T}}$. After stating the vector position of the obstacle, we can define the obstacle direction, $\mathbf{d}_o$, such as

$$\mathbf{d}_o = \frac{\mathbf{q}_r - \mathbf{q}_o}{\|\mathbf{q}_r - \mathbf{q}_o\|}. \tag{6}$$

In equation (6), $\|\mathbf{q}_r - \mathbf{q}_o\|$ is the magnitude of a vector difference between the robot position and the obstacle. Since we have the direction of the obstacle, we can determine the repulsive force. Let there be n number of obstacles, then the repulsive force, $\mathbf{F_r}$, can be denoted as

$$\mathbf{F_r} = \frac{k_r}{(d - d_s + \epsilon)^2}\mathbf{d}_o \tag{7}$$

where k_r, d, and d_s represent the repulsive gain, the distance between the robot and the obstacle, and the safety distance between the robot and the obstacle, respectively. Here, the term d_s refers to the maximum distance between the robot and the obstacle at which the repulsive force still has an effect. It should be noted that d_s is given. Additionally, we also have ϵ, which is a small constant necessary to avoid division by zero.

C. Total Force

Once the forces have been determined, they can be combined by summation to obtain the total force. It is assumed that there are n obstacles, then the total force can be denoted as

$$\mathbf{F_{t1}} = \mathbf{F_{a1}} + \sum_{i=1}^{n+1} \mathbf{F_r}_i, \tag{8}$$

$$\mathbf{F_{t2}} = \mathbf{F_{a2}} + \sum_{i=1}^{n} \mathbf{F_r}_i, \tag{9}$$

where $\mathbf{F_{t1}}$ is the total force for the leader-robot. Meanwhile, $\mathbf{F_{t2}}$ is the force for the follower-robot. The number of repulsive forces for the leader-robot is $n+1$ since we consider the follower-robot as a moving obstacle.

III. Local Minima and Perpendicular Force

In this part we will focus on discussing the local minima problem. The local minima problem due to SAROG (Symmetrically Aligned Robot-Obstacle-Goal) is briefly explained in subsection III-A. We also present an approach for escaping the local minima by using perpendicular force in subsection III-B.

A. Symmetrically Aligned Robot-Obstacle-Goal

Typically, the repulsive force is the primary cause of local minima in path planning. Consider a scenario where the magnitudes of the attractive and repulsive forces are equal, resulting in a resultant total force of zero. This occurrence is evident in configurations such as SAROG, where the robot, obstacle, and goal are aligned symmetrically. In such cases, the total force being equal to zero leads to local minima, causing the robot to become stuck and unable to move forward. A visualization depicting the local minima caused by SAROG configuration is presented in the Figure 1.

B. Perpendicular Force

The perpendicular force is needed for escaping the local minima. Here, the first need to do is to define the perpendicular direction, $\mathbf{d}_p$, such as

$$\mathbf{d}_p = \begin{cases} \begin{bmatrix} -y_o & x_o \end{bmatrix}^{\mathrm{T}} & \text{, if moving to the right,} \\ \begin{bmatrix} y_o & -x_o \end{bmatrix}^{\mathrm{T}} & \text{, if moving to the left.} \end{cases} \tag{10}$$

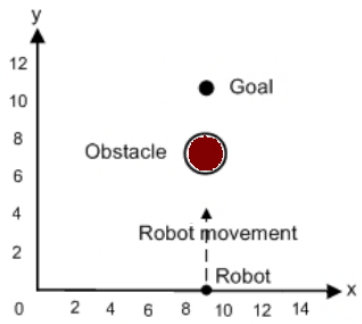

Fig. 1 Local minima caused by SAROG configuration.

We can redirect the robot to the right side of the obstacle by considering the negative of the $y-$coordinate and the $x-$coordinate of the obstacle direction vector as the perpendicular direction $\mathbf{d}_p$. On the contrary, if we want to redirect the robot to the left side of the obstacle, we can modify the perpendicular direction by taking the $y-$coordinate and the negative of the $x-$coordinate of the obstacle direction vector.

Now, we can calculate the perpendicular force as

$$\mathbf{F_p} = \frac{k_r}{(d - d_s + \epsilon)^2}\mathbf{d}_p. \tag{11}$$

Now, since we have the perpendicular force, we need to modify the total forces in equation (8) and (9). Hence, the mofified total forces can be denoted as

$$\mathbf{F_{t1}} = \mathbf{F_{a1}} + \sum_{i=1}^{n+1}\mathbf{F_{r}}_i + \sum_{i=1}^{n+1}\mathbf{F_{p}}_i, \tag{12}$$

$$\mathbf{F_{t2}} = \mathbf{F_{a2}} + \sum_{i=1}^{n}\mathbf{F_{r}}_i + \sum_{i=1}^{n}\mathbf{F_{p}}_i. \tag{13}$$

IV. Results and Analysis

In this section, we present two scenarios using numerical simulations. The first scenario in subsection IV-A focuses on verifying the effectiveness of the modified total force in overcoming local minima caused by SAROG. Later, the second scenario is presented in subsection IV-A. Here, the simulations are performed to establish the feasibility of the proposed method for a leader-follower system.

A. First Scenario

Before proceeding further, we need to define the parameters for the numerical simulations. The number of iterations for both scenario is 100. In the first scenario, we use $k_{a1} = 1$ and $k_r = 100$. The initial position of the robot is at $\mathbf{q}_l(0) = \begin{bmatrix} 0 & 0 \end{bmatrix}^{\mathrm{T}}$ and the goal is locataed at $\mathbf{q}_g = \begin{bmatrix} 100 & 100 \end{bmatrix}^{\mathrm{T}}$. In the same time, there are three obstacles as depicted at Figure 2 and 3. Here we define a condition, if the distance between the last generated path and the goal is less than 2 units for given iterations, then it is a success. Otherwise, the method fails to meet the requirement.

The main objective of this scenario is to reach the goal while escaping the local minima due to SAROG. First, we conduct the numerical simulation for the initial APF without the perpendicular force using the mentioned parameters. The result is depicted in Figure 2, that illustrates how the APF fails accomplish the task.

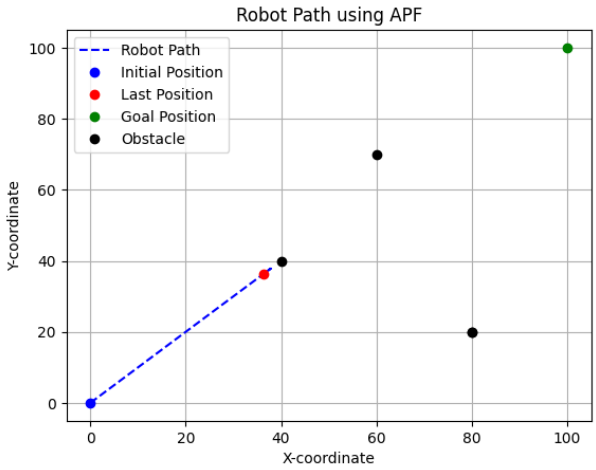

Fig. 2 APF unable to escape from local minima due to SAROG.

In Figure 2, we can see that the generated path unable to reach the goal. Furthermore, it stucks and unable to escape from local minima. This problem arises because of the SAROG configuration, which causes the attractive force and repulsive force to nullify each other. Henceforth, the total force $\mathbf{F_{t1}}$ becomes zero. In order to overcome this issue, we introduce the modified APF using the perpendicular force. Here, we decide the perpendicular direction to be $\mathbf{d}_p = \begin{bmatrix} -y_o & x_o \end{bmatrix}^{\mathrm{T}}$. It implies that the generated path will be redirected to the right side.

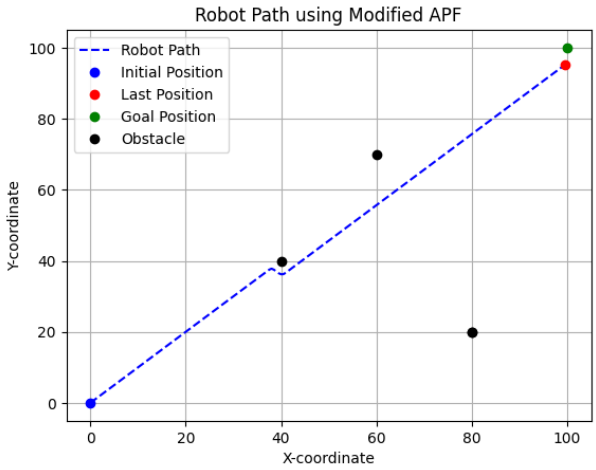

Fig. 3 Modified APF prevails escaping from local minima.

Based on Figure 3, it can be stated that the modified APF using perpendicular force succeeds on accomplishing the task for reaching the goal while escaping the local minima. It achieves the feat by moving to the right side, which is decided by the perpendicular direction $\mathbf{d}_p$. It is also possible to move the left side by adjusting the configuration of $\mathbf{d}_p$.

Although the decision of the perpendicular direction (whether to redirect to the right or left side) can be arbitrary, it is preferable to have an understanding of the entire map. This allows us to determine which direction is less obstructed by obstacles. In this scenario, the right side is favored as it is observed to be less obstructed compared to the other side.

B. Second Scenario

In the first scenario, it is verified that the proposed method serves a solution for escaping the local minima. Henceforth, in the second scenario it will be deployed for leader-follower system. There are three conditions that indicate the effectiveness of the proposed method for the system. First, the proposed method must be implemented for both the robots to successfully escape local minima caused by SAROG. This ensures that the robots can navigate away from obstacles and overcome any potential stuck points. Second, the distance between the generated path for the leader-robot and the goal must be within a tolerated distance. It ensures that the leader-robot is progressing to the goal. It is similar for the third condition, the distance between the generated path for the follower-robot and the path of the leader-robot must be within a tolerated distance. It ensures that the follower-robot can stay in close proximity to the leader-robot and follow it.

It is similar to the first one, we need to define the parameters of the numerical simulation for this scenario as well. Here, the parameters $k_{a1} = 1$, $k_{a2} = 1$, $k_r = 100$. The initial position of the leader-robot is at $\mathbf{q}_l(0) = \begin{bmatrix} 0 & 0 \end{bmatrix}^{\mathrm{T}}$ while the follower is positioned at $\mathbf{q}_f(0) = \begin{bmatrix} 10 & 10 \end{bmatrix}^{\mathrm{T}}$. The goal itself is located at $\mathbf{q}_g = \begin{bmatrix} 40 & 40 \end{bmatrix}^{\mathrm{T}}$. As long as the path generated for the leader-robot is close enough to the goal within a certain tolerance, it can be concluded that the goal is reachable. Here the tolerance is 2 units. Meanwhile, the obstacles are stationary occupying four points on the map. The results of numerical simulation in this scenario is presented in Figure 4.

Based on Figure 4, it is obvious that both leader and follower-robot are move to the right side to avoid the obstacle. They prevail on escaping the local minima caused by SAROG. It can be achieved by assigning $\mathbf{d}_p = \begin{bmatrix} -y_o & x_o \end{bmatrix}^{\mathrm{T}}$. The reason why we decide it needs to be redirected to the right side is due to the fact that the goal is located in the upper-right side (Northeast) from the initial position of the leader-robot.

The second condition is also satisfied as verified in Figure 5. Based on Figure 5, we can see that the distance between the generated path for the leader and the goal is shrinking over the time. Nevertheless, after more than 50 iterations, the distance between them does not change. It indicates that the generated path has reached the the tolerated distance, which is 2 units.

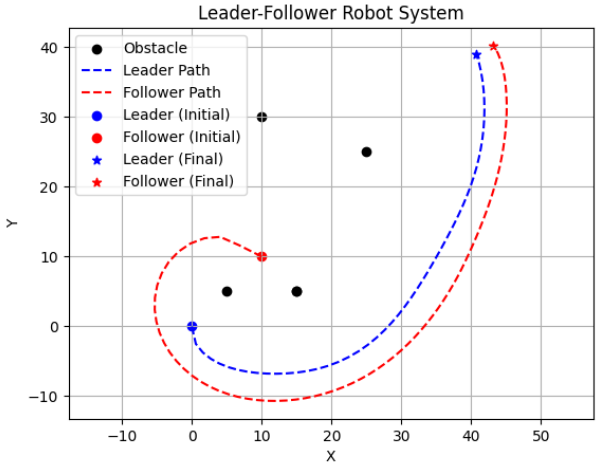

Fig. 4 Modified APF for Leader-Follower system.

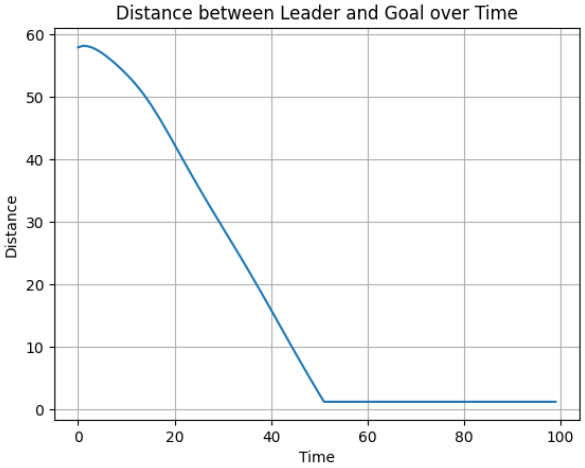

Fig. 5 Distance between leader-robot and goal over the time.

Lastly, the third condition, the distance between the leader and follower, is also satisfied. We can see in Figure 6, that the distance is unchanged at 2 units after more than 70 iterations. There are several things that can be noticed from Figure 6. Apparently, while the path for the leader has not reached the goal, then the distance between leader and follower is keep increasing. After more than 50 iterations, the path generated for the leader is stopped. It is caused by the fact that the goal has been reached. On the other hand, the follower still chasing the leader and the distance is gradually decreasing over the time. It keeps decreasing untill it reaches the tolerated distance, which is 2 units after more than 70 iterations.

Since all of the conditions are satisfied, it can be concluded that the modified APF utilizing perpendicular force is suitable for implementation in a leader-follower system. It prevails on escaping the local minima and guides both the leader and follower-robot to their designated positions by also considering a safety distance between both of them.

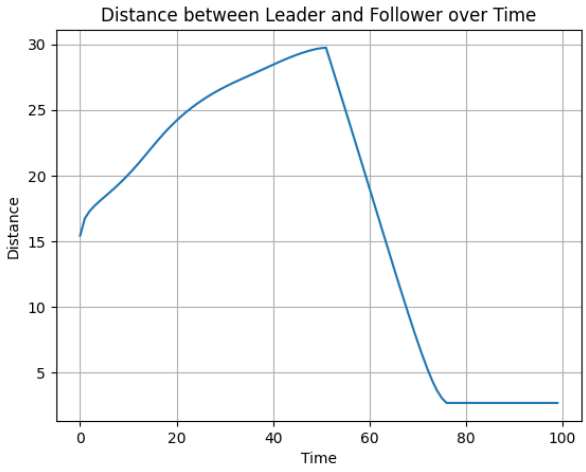

Fig. 6 Distance between leader-robot and follower-robot over the time.

V. Conclusion

In this paper, a modified artificial potential field by introducing the perpendicular force for the leader-follower system is presented. The perpendicular force is necessary for escaping the local minima caused by SAROG for both leader and follower-robot. The effectiveness of our proposed method is validated by numerical simulations in two different scenarios. The first scenario is conducted to verify the capability of perpendicular force for escaping the local minima. The results show that it prevails in generating the path to reach the goal, despite SAROG configurations. Later, in the second scenario, the goal is reached by the leader while being tracked by the follower.

References

[1] A. R. Khan, A. T. Khan, M. Salik, and S. Bakhsh, "An optimally configured hp-gru model using hyperband for the control of wall following robot," *International Journal of Robotics and Control Systems*, vol. 1, no. 1, pp. 66–74, 2021.

[2] Lasmadi, A. Cahyadi, S. Herdjunanto, and R. Hidayat, "Inertial navigation for quadrotor using kalman filter with drift compensation," *International Journal of Electrical and Computer Engineering*, vol. 7, no. 5, pp. 2596–2604, 2017.

[3] E. W. Dijkstra, "A note on two problems in connexion with graphs," *Numerische Mathematik*, vol. 1, no. 1, pp. 269–271, 1959.

[4] O. Khatib, "Real-time obstacle avoidance for manipulators and mobile robots," *International Journal of Robotics Research*, vol. 5, no. 1, pp. 90–98, 1986.

[5] S. M. LaValle and J. J. Kuffner Jr., "Randomized kinodynamic planning," *International Journal of Robotics Research*, vol. 20, no. 5, pp. 378–400, 2001.

[6] P. E. Hart, N. J. Nilsson, and B. Raphael, "A formal basis for the heuristic determination of minimum cost paths," *IEEE Transactions on Systems Science and Cybernetics*, vol. 4, no. 2, pp. 100–107, 1968.

[7] S. A. Gunawan, G. N. P. Pratama, A. I. Cahyadi, B. Winduratna, Y. C. H. Yuwono, and O. Wahyunggoro, "Smoothed a-star algorithm for nonholonomic mobile robot path planning," in *2019 International Conference on Information and Communications Technology (ICOIACT)*, 2019, pp. 654–658.

[8] O. Khatib, "Real-time obstacle avoidance for manipulators and mobile robots," in *Proceedings. 1985 IEEE International Conference on Robotics and Automation*, vol. 2, 1985, pp. 500–505.

[9] K. Nakazawa, K. Takahashi, and M. Kaneko, "Unified environment-adaptive control of accompanying robots using artificial potential field," in *2013 8th ACM/IEEE International Conference on Human-Robot Interaction (HRI)*, 2013, pp. 199–200.

[10] M. H. Mabrouk, "Crowd behavior simulation using artificial potential fields," *IAENG International Journal of Computer Science*, vol. 40, no. 4, pp. 220–229, 2013.

[11] A. A. A. Rizqi, A. I. Cahyadi, and T. B. Adji, "Path planning and formation control via potential function for uav quadrotor," in *2014 International Conference on Advanced Robotics and Intelligent Systems (ARIS)*, 2014, pp. 165–170.

[12] H. H. Triharminto, O. Wahyunggoro, T. B. Adji, and A. I. Cahyadi, "An integrated artificial potential field path planning with kinematic control for nonholonomic mobile robot," *International Journal on Advanced Science, Engineering and Information Technology*, vol. 6, no. 4, pp. 410–418, 2016.

[13] H. H. Triharminto, O. Wahyunggoro, T. B. Adji, A. I. Cahyadi, and I. Ardiyanto, "A novel of repulsive function on artificial potential field for robot path planning," *International Journal of Electrical and Computer Engineering*, vol. 6, no. 6, pp. 3262–3275, 2016.

[14] H. H. Triharminto, O. Wahyunggoro, T. B. Adji, A. Cahyadi, I. Ardiyanto, and Iswanto, "Local information using stereo camera in artificial potential field based path planning," *IAENG International Journal of Computer Science*, vol. 44, no. 3, pp. 316–326, 2017.